Accepted Manuscript

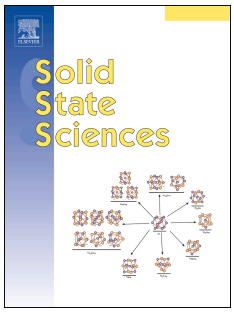

On the presence of antisite defect in monoclinic Li_2FeSiO_4 – A combined X-Ray diffraction and DFT study

Miloš D. Milović, Dragana D. Vasić Anićijević, Dragana Jugović, Vladan J. Anićijević, Ljiljana Veselinović, Miodrag Mitrić, Dragan Uskoković

PII: S1293-2558(18)30833-1

DOI: https://doi.org/10.1016/j.solidstatesciences.2018.11.008

Reference: SSSCIE 5793

To appear in: *Solid State Sciences*

Received Date: 1 August 2018

Revised Date: 29 October 2018

Accepted Date: 14 November 2018

Please cite this article as: Miloš.D. Milović, D.D. Vasić Anićijević, D. Jugović, V.J. Anićijević, L. Veselinović, M. Mitrić, D. Uskoković, On the presence of antisite defect in monoclinic Li_2FeSiO_4 – A combined X-Ray diffraction and DFT study, *Solid State Sciences* (2018), doi: https://doi.org/10.1016/j.solidstatesciences.2018.11.008.

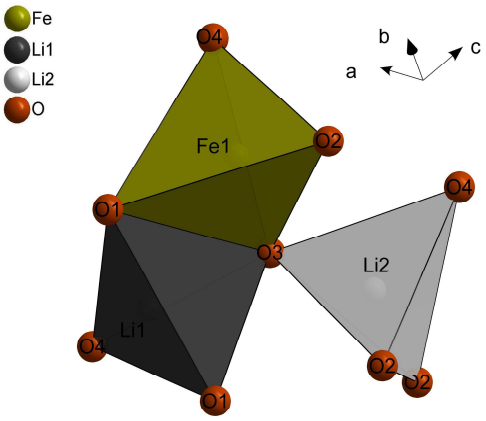

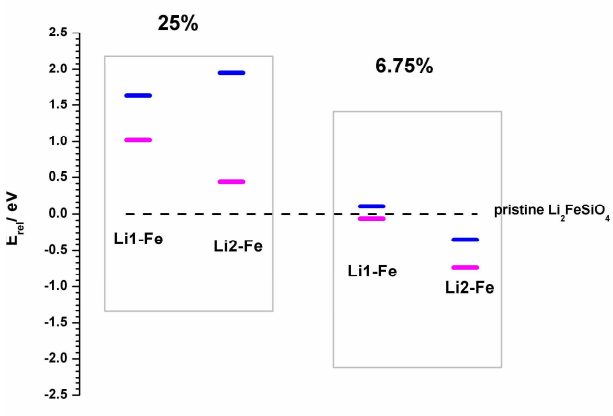

On the presence of antisite defect in monoclinic Li_2FeSiO_4 – a combined X-Ray Diffraction and DFT study

Miloš D. Milović[1,*], Dragana D. Vasić Anićijević[2], Dragana Jugović[1], Vladan J. Anićijević[3], Ljiljana Veselinović[1], Miodrag Mitrić[2], Dragan Uskoković[1]

[1]Institute of Technical Sciences of SASA, Knez Mihailova 35/IV, 11 000 Belgrade, Serbia

[2]Vinča Institute of Nuclear Sciences, University of Belgrade, P.O. Box 522, 11 001 Belgrade, Serbia

[3]University of Belgrade – Faculty of Physical Chemistry, Studentski trg 12-16, 11158 Belgrade, Serbia

Keywords:

Li_2FeSiO_4; antisite defect; Rietveld method; DFT method.

Abstract

Li_2FeSiO_4 material, which was prepared by a solid state method, crystallized as monoclinic $P2_1/n$ polymorph. X-ray diffraction analysis with Rietveld structural refinement indicates specific occupation of Li2 crystallographic site by Fe^{2+} cation in the amount of 6 atom percents as a result of an antisite defect formation. The exlusive occupation of Li2 position, out of two crystallographic positions Li1 and Li2, by Fe^{2+} was discussed in relation to the differences that exist in the crystal environment of these positions and further investigated by DFT calculations. It was confirmed that Fe-Li2 substitution is energetically favorable compared to both Fe-Li1 substitution and the pristine crystal. In addition, changes of lattice geometry upon antisite defect formation were analyzed, and the obtained result is discussed in light of various factors (electronic, geometrical and enthropic) that contribute to the overall stability of the system.

1. Introduction

Compounds from the family of lithium transition-metal orthosilicates, with the general formula Li_2TmSiO_4, attract attention of researchers for possible cathode application in lithium ion batteries due to their potential to extract two Li-ions per formula unit, which would lead to the increased cathode capacity and energy density [1]. Thanks to the natural abundance of iron and more stable cycling performance, Li_2FeSiO_4 takes a prominent position in this group of compounds. Li_2FeSiO_4 builds tetrahedral structures with all the cations located within 1/2 of tetrahedral sites of a slightly distorted hexagonally-close-packed lattice of oxygen; a possible different orientation and interconnection of tetrahedra results with several polymorph structures reported, with *Pmn*2_1, *P*2_1/*n* and *Pmnb* symmetry [2]. Upon first cycles of charge-discharge, Li_2FeSiO_4 is susceptible to a structural change which includes cation disordering and defect formation: namely, the formation of an antisite defect was observed, where Li^+ and Fe^{2+} exchange their crystallographic positions (and even in large concentrations of around 50% of the exchange) [3,4]. There are also reports on a new phase formation upon cycling, inverse *Pmn*2_1 phase [5]; in inverse *Pmn*2_1 structure, the site normally occupied by Fe^{2+} is occupied exclusively by Li^+, while remaining Li^+ share its sites with Fe^{2+}, and therefore inverse *Pmn*2_1 phase is inherently disordered. Density functional theory investigations support these findings. DFT showed that full reversal of Li/Fe site occupations is energetically favored on delithiation for all three electrochemically active Li_2FeSiO_4 polymorphs [6]. Lu et al. pointed that formation of Li-Fe antisites can induce a metastability competition between monoclinic and orthorhombic phases, with neither dominating across nearly the entire discharging profile from Li_2FeSiO_4 through to $LiFeSiO_4$ [7].

Even as synthesized, uncycled, Li_2FeSiO_4 material is prone to antisite defect formation (although in smaller concentrations) [3,8], which can be desirable in order to reduce stress that material suffers during first cycles [9]. In our earlier work, the antisite defect in concentration of 5 atom% was detected in the monoclinic *P*2_1/*n* polymorph of Li_2FeSiO_4 which was prepared by a solid state reaction as Li_2FeSiO_4/C composite [10]. X-ray diffraction and Mössbauer spectroscopy analysis of the obtained Li_2FeSiO_4/C powder revealed exclusive occupation of Li2 crystallographic position (out of two possible positions, Li1 and Li2) by Fe as a result of the antisite present. This conclusion, which was not spotted in the literature elsewhere, encouraged us to perform a more detailed study considering particularly the properties of the antisite defect.

In this paper, Li_2FeSiO_4 powder with monoclinic *P*2_1/*n* structure was synthesized by means of a conventional solid state reaction with no organic precursor involved. Therefore, the obtained product contains no carbon which is (although beneficial for the electrochemical performance) superfluous for the structural examination of the active material. The powder was characterized by X-ray diffraction with a special attention paid to the crystal structure refinement. The results of the X-ray diffraction analysis were compared with theoretical calculations carried out by DFT method in order to provide a systematic insight into the nature of the observed defect.

2. Methodology

2.1 Experimental

Li_2FeSiO_4 was synthesized via solid state reaction with the following chemicals. Iron(III) nitrate nonahydrate ($Fe(NO_3)_3 \cdot 9H_2O$, ACS, 98.0-101.0 %) and lithium carbonate (Li_2CO_3, ACS, 99.0 % min) were purchased from Alfa Aesar. Amorphous silicon dioxide (SiO_2, >99.8%, CAB-O-SIL®) was provided from Cabot Co. Starting compounds of $Fe(NO_3)_3 \cdot 9H_2O$, Li_2CO_3 and SiO_2 were mixed in equimolar amounts, dispersed in distilled water, ground after drying and then calcined for 2 h at the temperature 750 °C in a flowing, slightly reductive atmosphere (Ar + 5% H_2, flow rate ≈ 0.1 dm^3 min^{-1}).

The X-ray powder diffraction measurements were performed on a Philips PW 1050 X-ray powder diffractometer using Ni-filtered Cu Kα radiation and Bragg-Brentano focusing geometry. The diffraction intensity was recorded in the 2θ range of 10-120° with a step size of 0.02° and a counting time of 15 s per step. The Rietveld refinement of the Li_2FeSiO_4 crystal structure was performed using the *FullProf* computer program in the *WinPLOTR* environment.

2.2 Computational

Density functional calculations are performed using the Vanderbilt ultra-soft pseudo-potentials [11] and plane wave basis sets as implemented in Quantum Espresso (QE) [12]. The GGA-PBE approximation for exchange-correlation functional [13] with Hubbard correction (GGA+U) was used in simplified version of Cococcioni and de Gironcoli [14]. An effective U value of 4.5 eV for the Fe-d states is taken from the literature [15]. The plane wave kinetic energy cutoff was set to 30 Ry, and charge density cutoff was 480 Ry. Convergence criterion for self-consistency was set to 10^{-6} Ry, and force convergence threshold for ionic minimization in geometry optimization was set to $1.5x10^{-4}$ eV/Å. Marzari-Vanderbilt [16] smearing was used to improve convergence. All calculations were spin polarized. The k-point grid was sampled through Monkhorst - Pack scheme [17]. Calculations for pristine crystal and 25% Li-Fe interchange were performed in a 32 atom supercell with k-point grid 4x4x4, and calculations for 6.75% Li2-Fe interchange were performed in a 128-atom supercell, with k-point grid 2x2x4. Both cells are represented in Figure S1.

3. Results and discussion

3.1 Rietveld analysis

The synthesized powder of Li_2FeSiO_4 crystallized, and was refined (Figure 1), in the monoclinic $P2_1/n$ space group (#14) with the structure where Li^+ ions occupy two, Fe^{2+} ions occupy one, Si^{4+} ions occupy one and O^{2-} ions occupy four different general 4e crystallographic positions [x, y ,z] as presented in Tables 1 and 2. Besides monoclinic Li_2FeSiO_4 phase X-ray diffraction measurement revealed traces of Li_2SiO_3 impurity phase

(orthorhombic space group $Cmc2_1$, #36). The obtained lattice and structural parameters for Li_2FeSiO_4 represented in the standard setting $P2_1/c$ are given in Table S1.

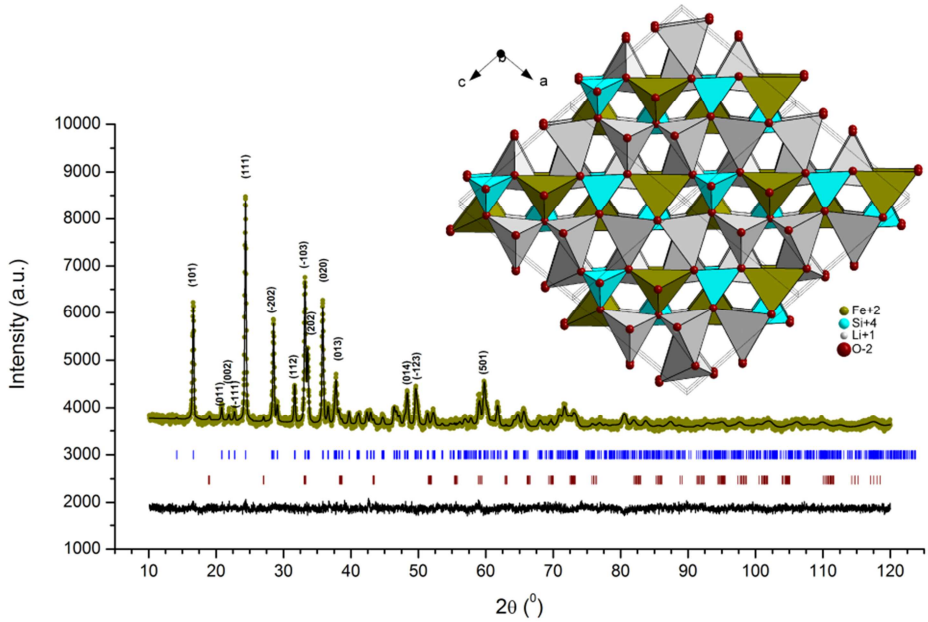

Figure 1. The observed (green dots), calculated (black line) and difference (bottom black line) X-ray diffraction data of the Li_2FeSiO_4 powder taken at room temperature. Vertical markers below the diffraction patterns indicate positions of possible Bragg reflections for the monoclinic Li_2FeSiO_4 (blue) and orthorhombic Li_2SiO_3 (red). Tetrahedral structure of the monoclinic $P2_1/n$ Li_2FeSiO_4 is shown as inset.

Table 1. The main results of the Rietveld refinement.

Lattice parameters	a = 8.2331(12) Å
	b = 5.0170(5) Å
	c = 8.2295(11) Å
	β = 99.099(4) °
Cell volume (Å^3)	335.65(7)
Fraction of Li_2SiO_3 (wt%)	2.3(2)
Li2-site occupation by Fe	0.060(3)
R_{wp} factor (%)	17.1

Table 2. Refined atomic fractional coordinates, temperature factors and site occupations in the $P2_1/n$ Li_2FeSiO_4 structure.

Atomic position	Wyckoff symbol	Fractional coordinates			B (Å^2)	Occ.
		x	y	z		
Li1	4e	0.645(7)	0.854(8)	0.746(6)	2.8(10)	1.0
Li2	4e	0.594(4)	0.199(7)	0.078(4)	1.66(12)	0.940(3)
Fe1	4e	0.289(1)	0.7995(9)	0.5428(9)	1.66(12)	0.940(3)
Li3	4e	= Fe1	= Fe1	= Fe1	1.66(12)	0.060(3)
Fe2	4e	= Li2	= Li2	= Li2	1.66(12)	0.060(3)
Si	4e	0.039(1)	0.817(2)	0.799(2)	1.46(19)	1.0
O1	4e	0.884(3)	0.737(5)	0.811(3)	2.09(18)	1.0
O2	4e	0.401(3)	0.218(3)	0.898(3)	2.09(18)	1.0
O3	4e	0.679(3)	0.761(3)	0.438(3)	2.09(18)	1.0
O4	4e	0.964(3)	0.878(3)	0.212(3)	2.09(18)	1.0

The obtained results are in good agreement with those obtained in our previous work [10], also implying that an antisite defect is formed. During refinement procedure, additional electron density at Li2 crystallographic site was indicated by obtaining negative value of B temperature factor (or by obtaining occupation parameter over 1, depending what is allowed to vary) for Li^+ ion at this position, strongly suggesting partial replacement of Li^+ by some larger ion. At first, an overall B factor was refined and the obtained value was set as starting value for each of the atoms. The B factors for the O atoms were constrained and refined together. If allowed to vary freely, the B factor tends to rise very high for the Fe atom, while at the same time for Li2, B factor tends to decrease to a negative value. For this reason, new atomic positions were created in the input file: Li3 and Fe2, representing Li at Fe1 position and Fe at the Li2 position, respectively, and their occupational parameters were included in the refinement (Table 2). In addition, B factors for Fe and Li2 were constrained and refined as one. A noticeable decrease of R values and the best refinement was achieved with the arrangement where 6 atom% of Fe^{2+} occupy Li2 crystallographic position only. Also, later during the refinement it was allowed for Fe^{2+} ions to occupy, besides Fe site, both Li1 and/or Li2 site. For comparison, the obtained R_{wp} factors of the refinement with: no antisite included, Fe-Li1 antisite, mixed Fe-Li1/Li2 antisite and Fe-Li2 antisite were 18.5, 18.4, 17.7 and 17.1, respectively.

The result that Fe^{2+} occupies Li2 position exclusively out of two possible positions Li1 and Li2 must have come as a consequence of the specific geometries of Li1 and Li2 crystallographic positions. The refined fractional atomic coordinates from Table S1 were used for the calculation of all relevant bond distances that enabled us to determine coordination polyhedra. In $P2_1/n$ structure of Li_2FeSiO_4, LiO_4 tetrahedra form layers which alternate with

the layers of SiO_4 and FeO_4 along [101] direction (Figure 1 inset). The main differences between Li1 and Li2 tetrahedral sites in relation to the neighboring tetrahedra are as follows. Each $Li1O_4$ tetrahedron shares one common edge with one FeO_4 tetrahedron and shares corners with two FeO_4, two $Li1O_4$, two $Li2O_4$ and four SiO_4 tetrahedra (Figure 2a). And each $Li2O_4$ shares one common edge with one $Li2O_4$ and shares corners with two $Li1O_4$, four FeO_4 and four SiO_4 tetrahedra (Figure 2b). Therefore, the only edge-sharing pairs of tetrahedra in $P2_1/n$ polymorph structure are $Li1O_4/FeO_4$ and $Li2O_4/Li2O_4$. The arrival of Fe on Li1 site would result in, according to the Pauling's rule #3 [18], unfavorable configuration where two adjacent FeO_4 tetrahedra share a common edge. As a result of that, the energy of the system rises. On the other side, if substitution takes place on Li2 site more stable configuration would be accomplished where FeO_4 only shares corners with the neighboring FeO_4 tetrahedra.

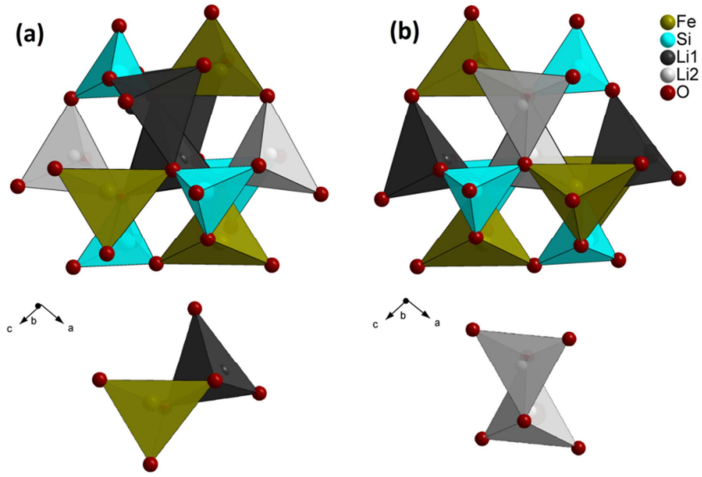

Figure 2. Crystal environment of Li1 (a) and Li2 tetrahedral site (b); the edge sharing pairs of tetrahedra are shown as insets.

3.2 DFT calculations

In order to confirm that antisite defect occurs exclusively as Fe-Li2 interchange, system was further investigated by DFT calculations. Spin polarized calculations for the pristine crystal have shown that antiferromagnetic state is slightly preferential over ferromagnetic (about 9 meV per elementary cell). This is in good agreement with experimental observation for lithium iron silicates (antiferromagnetic to paramagnetic transition at T<20 K) [19] and previous DFT calculations for similar systems [7, 20]. According to this, all further calculations are performed in antiferromagnetic state. Determination of lattice parameters has been performed for pristine crystal, and the crystal with Fe-Li2 interchange defect at concentration 6.75%, which is very close to the defect concentration obtained from Rietveld analysis. Optimized lattice parameters are shown in Table 3.

Table 3. Lattice parameters calculated by DFT, for pristine Li_2FeSiO_4 and 6.75% Fe-Li2 interchange.

	a /Å	b/Å	c / Å	β / °
pristine	8.369	5.109	8.394	99.43
Li2-Fe 6.75%	8.377	5.122	8.401	98.75

Presented results are comparable with those calculated from XRD data. An overestimation of lattice parameters of pristine crystal, of about 1-2% is expected within DFT-GGA approximation. An additional strain is obvious when a defect is introduced, resulting in a further increase of lattice parameters a, b and c. Such result confirms that the formation of the defect is followed by a noticeable structural change, which affects at least the elementary cell containing the defect and its nearby environment.

In addition, fractional atomic coordinates from DFT optimized lattice of the crystal with 6.75% Fe-Li2 interchange are calculated and presented in Table 4. As the calculation supercell contains 4 elementary cells (E.C.) and one of them contains a defect, both E.C. containing the defect and the E.C. on the counter side of the supercell are given.

Table 4. DFT optimized fractional coordinates of the crystal with 6.75% Fe-Li2 interchange. Elementary cell (defect E.C. or counter E.C.) that coordinate data refer to is marked in the insert figure by orange rectangle.

	Defect E.C.			**Counter E.C.**		
	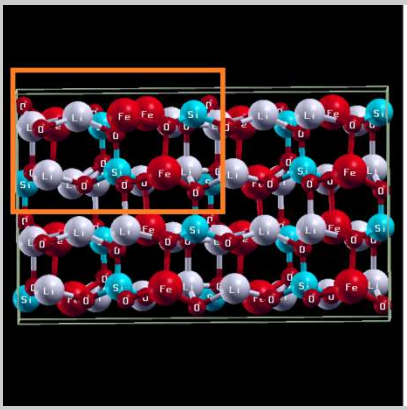			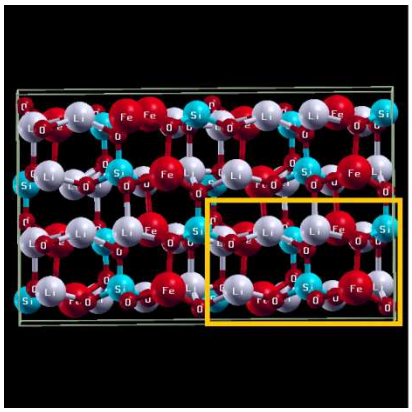		
	x	y	z	x	y	z
Li1	0.662390	0.788881	0.670865	0.667098	0.787095	0.672256
Li2	0.585824	0.196172	0.089889	0.583010	0.198992	0.083247
Li3	0.297674	0.805627	0.547392	---	----	---
Fe1	0.291940	0.803138	0.540722	0.296608	0.803860	0.546679
Fe2	0.581330	0.205527	0.082765	---	---	---
Si	0.044801	0.806567	0.789186	0.042326	0.807298	0.791151
O1	0.865767	0.692570	0.822010	0.866212	0.691448	0.821528
O2	0.418028	0.195631	0.881844	0.418274	0.202377	0.885243
O3	0.686760	0.787606	0.433133	0.685918	0.787726	0.434898
O4	0.965373	0.872008	0.214875	0.963296	0.872733	0.212233

Generally a good agreement between DFT and refined fractional coordinates is achieved. Most considerable differences (about 0.5-1 Å) between refined and DFT calculated atomic positions are observed for the Li1 and Li2 atoms. Due to the low X-ray atomic scattering factors of lithium, detection and precise determination of its atomic position by X-ray

diffraction is difficult. For the same reason, examination of Li atoms occupation at Fe sites by XRD was not possible. Although expected, the latter result emphasizes the complementarity of used techniques (XRD and DFT) in the investigation of this and similar systems. As can be seen from Table 4, differences between Li2 and Fe2 (as well as Li3 and Fe1) positions in defect E.C. are small – about 0.05Å Moreover, local differences in fractional coordinates between defect E.C. and counter E.C. in the supercell are very small, staying within the range of about 0.01 Å. In brief, DFT calculations within our model point to the long range strain as the main effect of Fe-Li2 antisite defect formation, while local structure rearrangement (i.e. significant rearrangement of ions within the defect E.C. and in its nearby environment) was not obtained.

The energetics of the formation of antisite defect by Fe-Li interchange was investigated at defect concentrations of 25 molar % and 6.75% (which is close to the concentration 6.0% which is determined by Rietveld refinement). Both Fe-Li2 and Fe-Li1 substitution were examined. When the interchange of ions in crystal lattice is performed, the calculated total energy change can generally be divided into 1) electronic contribution, that originates from the change of electronic and magnetic interactions and 2) geometrical contribution, originating from the subsequent geometry optimization:

$$E_{rel} = E_{system} - E_{pristine} = E_{electronic} + E_{geometrical} \quad (1)$$

where E_{rel} is total energy change upon introduction of the defect; E_{system} – total energy of an elementary cell of a defect crystal; $E_{pristine}$ – total energy of an elementary cell of pristine crystal; $E_{electronic}$ – electronic contribution to the energy change upon defect formation; $E_{geometrical}$ – contribution to the energy change upon geometry optimization after defect formation.

Electronic contribution is calculated as the energy difference between the fully optimized pristine crystal, and the crystal where interchanged ions are fixed at the positions that are optimized for the pristine crystal:

$$E_{electronic} = E_{fixed} - E_{pristine} \quad (2)$$

E_{fixed} – total energy of the cell where interchanged ions are fixed at the positions that are optimized for the pristine crystal. Any further energy decrease upon geometry optimization is ascribed to geometrical contribution:

$$E_{geometrical} = E_{system} - E_{fixed} \quad (3)$$

Such obtained electronic and relaxation contributions are presented in Figure 3.

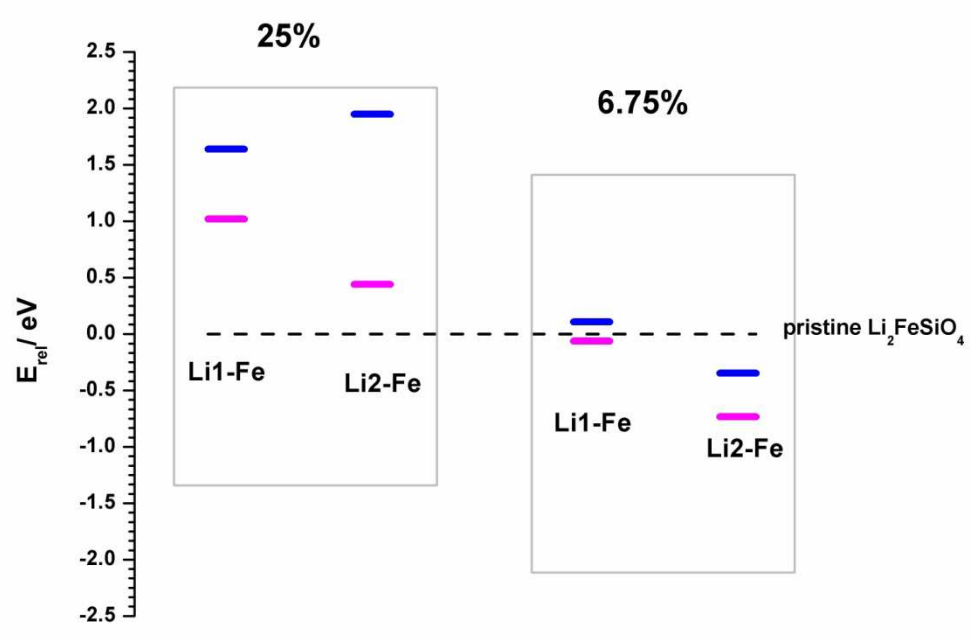

Figure 3. DFT-GGA calculated electronic (royal blue dots) and relaxation (distance from royal blue to magenta dots) contributions to the total energy change upon formation of Li1-Fe and Li2-Fe antisite defect, in concentrations 25% and 6.75%. All energies are normalized to one elementary cell. Energy of the fully optimized elementary cell of pristine Li_2FeSiO_4 is taken as a reference, and total energy change upon defect formation (E_{rel}) is given in the ordinate.

As expected from Rietveld data, Li2-Fe is significantly more stable than Li1-Fe for both investigated defect concentrations. In case of 25% Li-Fe interchange, the crystal stays destabilized compared to the pristine state even after relaxation, in both Li1-Fe and Li2-Fe cases, by at least 0.4 eV. Interestingly, Li2-Fe lattice is rather more stabilized by relaxation compared to Li1-Fe. On the other hand, for 6.75% Li2-Fe interchange a significant stabilization compared to pristine Li_2FeSiO_4 is obtained, being in a good agreement with experimental observation that Li2-Fe defect is formed in concentration about 6%. Moreover, it can be noticed that the formation of Li2-Fe defect is thermodynamically favorable by 0.34 eV compared to pristine crystal, even without relaxation. The latter result points also to the remarkable role of electronic interactions as the driving force for Li2-Fe antisite defect formation. This is obviously not the case for Li1-Fe antisite, which exhibits no significant stabilization at all compared to the pristine crystal.

Besides the internal energy stabilization upon Fe-Li2 antisite defect formation, which is confirmed by DFT calculations, it can be proposed that the entropy of the system will increase with the formation of antisite defect compared to pristine crystal, further increasing the probability that the defect will be formed spontaneously. In order to estimate the configuration entropy increase upon antisite defect formation in amount of 6.75%, a simple statistical approach is applied. Configuration entropy change was calculated by taking into account the contribution of the defect formation (mixing of Li and Fe atoms at Li2 and Fe sites) to the Boltzmann's relation [21]:

$$\Delta S_{conf} = k_b \cdot \ln(W) = k_b \cdot \ln\left(\frac{N_{Li2}!}{(N_{Li2/Li})! \cdot (N_{Li2/Fe})!}\right)^2 \quad (4)$$

Where, k_b is the Boltzmann's constant and W is the number of possible arrangements; N_{Li2} is the number of Li2 positions (which equals the number of Fe positions); $N_{Li2/Li}$ is the number of Li2 positions occupied by lithium and $N_{Li2/Fe}$ is the number of Li2 positions occupied by iron. Calculated configuration entropy increase upon the formation of an antisite defect (6.75%) according to equation (4) is $11.95 \cdot 10^{-5}$ eV/K per crystal elementary cell, and the same value is obtained for Li1-Fe interchange. Details of configuration entropy calculation are provided in the supplementary data.

At the temperature 300 K, formation of the 6.75% antisite defect (both Li1-Fe and Li2-Fe) will result in an additional decrease of Gibbs free energy by 0.036 eV per elementary cell. Final estimation of Gibbs free energy change per elementary cell, upon defect formation at 300 K yields:

$$\Delta G^f_{Li2-Fe} = \Delta E^{Li2-Fe}_{rel} - T\Delta S'_{conf} = -0.734 \text{ eV} - 0.036 \text{ eV} = -0.770 \text{ eV} \quad (5)$$

$$\Delta G^f_{Li1-Fe} = \Delta E^{Li1-Fe}_{rel} - T\Delta S'_{conf} = -0.062 \text{ eV} - 0.036 \text{ eV} = -0.098 \text{ eV} \quad (6)$$

Where, $\Delta G^f_{Li1(2)-Fe}$ is the Gibbs free energy of the formation of Li1-Fe (Li2-Fe) antisite defect; $\Delta E^{Li1(2)-Fe}_{rel}$ is the DFT calculated total energy change upon Li1-Fe (Li2-Fe) antisite defect formation.

4. Conclusion

X-ray powder diffraction analysis of the prepared monoclinic $P2_1/n$ polymorph of Li_2FeSiO_4 indicates specific occupation of Li2 crystallographic site by Fe^{2+} cation in the amount of 6 atom percents as a result of an antisite defect formation. DFT calculations confirmed that Fe-Li2 substitution in the amount determined by Rietveld analysis is energetically favorable compared to both Fe-Li1 substitution and the pristine crystal by about 0.7 eV per elementary cell. Formation of the Li2-Fe antisite defect in concentration 6.75% is driven by both electronic and geometrical factors that determine the total energy of the system, and followed by a considerable lattice strain. On the other hand, it was shown that the formation of Fe-Li1 antisite of the same concentration is much less stabilized energetically, what is ascribed to an unfavorable configuration with the edge-sharing pairs of FeO_4/FeO_4 tetrahedra.

Acknowledgements

The Ministry of Education, Science and Technological Development of the Republic of Serbia provided financial support for this study under Grant Nos. III 45004 and III 45015.

References

[1] M.S. Islam, R. Dominko, C. Masquelier, C. Sirisopanaporn, A.R. Armstrong, P.G. Bruce, Silicate cathodes for lithium batteries: alternatives to phosphates?, J. Mater. Chem. 21 (2011) 9811. doi:10.1039/c1jm10312a.

[2] G. Mali, C. Sirisopanaporn, C. Masquelier, D. Hanzel, R. Dominko, Li_2FeSiO_4 Polymorphs Probed by ^{6}Li MAS NMR and ^{57}Fe Mössbauer Spectroscopy, Chem. Mater. 23 (2011) 2735–2744. doi:10.1021/cm103193a.

[3] A. Nytén, S. Kamali, L. Häggström, T. Gustafsson, J.O. Thomas, The lithium extraction/insertion mechanism in Li_2FeSiO_4, J. Mater. Chem. 16 (2006) 2266. doi:10.1039/b601184e.

[4] A. Kojima, T. Kojima, T. Sakai, Structural Analysis during Charge-Discharge Process of Li_2FeSiO_4 Synthesized by Molten Carbonate Flux Method, J. Electrochem. Soc. 159 (2012) A525–A531. doi:10.1149/2.jes112828.

[5] A.R. Armstrong, N. Kuganathan, M.S. Islam, P.G. Bruce, Structure and Lithium Transport Pathways in Li_2FeSiO_4 Cathodes for Lithium Batteries, J. Am. Chem. Soc. 133 (2011) 13031–13035. doi:10.1021/ja2018543.

[6] A. Liivat, Structural changes on cycling Li_2FeSiO_4 polymorphs from DFT calculations, Solid State Ion. 228 (2012) 19–24. doi:10.1016/j.ssi.2012.08.016.

[7] X. Lu, H.-C. Chiu, K.H. Bevan, D.-T. Jiang, K. Zaghib, G.P. Demopoulos, Density functional theory insights into the structural stability and Li diffusion properties of monoclinic and orthorhombic Li_2FeSiO_4 cathodes, J. Power Sources. 318 (2016) 136–145. doi:10.1016/j.jpowsour.2016.04.014.

[8] A. Boulineau, C. Sirisopanaporn, R. Dominko, A.R. Armstrong, P.G. Bruce, C. Masquelier, Polymorphism and structural defects in Li_2FeSiO_4, Dalton Trans. 39 (2010) 6310. doi:10.1039/c002815k.

[9] S. Ferrari, D. Capsoni, S. Casino, M. Destro, C. Gerbaldi, M. Bini, Electrochemistry of orthosilicate-based lithium battery cathodes: a perspective, Phys. Chem. Chem. Phys. 16 (2014) 10353. doi:10.1039/c4cp00511b.

[10] D. Jugović, M. Milović, V.N. Ivanovski, M. Avdeev, R. Dominko, B. Jokić, D. Uskoković, Structural study of monoclinic Li_2FeSiO_4 by X-ray diffraction and Mössbauer spectroscopy, J. Power Sources. 265 (2014) 75–80. doi:10.1016/j.jpowsour.2014.04.121.

[11] D. Vanderbilt, Soft self-consistent pseudopotentials in a generalized eigenvalue formalism, Phys. Rev. B. 41 (1990) 7892–7895. doi:10.1103/PhysRevB.41.7892.

[12] P. Giannozzi, S. Baroni, N. Bonini, M. Calandra, R. Car, C. Cavazzoni, D. Ceresoli, G.L. Chiarotti, M. Cococcioni, I. Dabo, A. Dal Corso, S. de Gironcoli, S. Fabris, G. Fratesi, R. Gebauer, U. Gerstmann, C. Gougoussis, A. Kokalj, M. Lazzeri, L. Martin-Samos, N. Marzari, F. Mauri, R. Mazzarello, S. Paolini, A. Pasquarello, L. Paulatto, C. Sbraccia, S. Scandolo, G. Sclauzero, A.P. Seitsonen, A. Smogunov, P. Umari, R.M. Wentzcovitch, QUANTUM ESPRESSO: a modular and open-source software project for quantum simulations of materials, J. Phys. Condens. Matter. 21 (2009) 395502. doi:10.1088/0953-8984/21/39/395502.

[13] J.P. Perdew, K. Burke, M. Ernzerhof, Generalized Gradient Approximation Made Simple, Phys. Rev. Lett. 77 (1996) 3865–3868. doi:10.1103/PhysRevLett.77.3865.

[14] M. Cococcioni, S. de Gironcoli, Linear response approach to the calculation of the effective interaction parameters in the LDA+U method, Phys. Rev. B, 71 (2005) 035105. doi:10.1103/PhysRevB.71.035105

[15] C. Eames, A.R. Armstrong, P.G. Bruce, M.S. Islam, Insights into Changes in Voltage and Structure of Li_2FeSiO_4 Polymorphs for Lithium-Ion Batteries, Chem. Mater. 24 (2012) 2155–2161. doi:10.1021/cm300749w.
[16] N. Marzari, D. Vanderbilt, A. De Vita, M.C. Payne, Thermal Contraction and Disordering of the Al(110) Surface, Phys. Rev. Lett. 82 (1999) 3296–3299. doi:10.1103/PhysRevLett.82.3296.
[17] H.J. Monkhorst, J.D. Pack, Special points for Brillouin-zone integrations, Phys. Rev. B. 13 (1976) 5188–5192. doi:10.1103/PhysRevB.13.5188.
[18] L. Pauling, The principles determining the structure of complex ionic crystals, J. Am. Chem. Soc. 51 (1929) 1010–1026. doi:10.1021/ja01379a006.
[19] M. Bini, S. Ferrari, C. Ferrara, M.C. Mozzati, D. Capsoni, A.J. Pell, G. Pintacuda, P. Canton, P. Mustarelli, Polymorphism and magnetic properties of Li_2MSiO_4 (M = Fe, Mn) cathode materials, Sci. Rep. 3 (2013) 3452. doi:10.1038/srep03452.
[20] P. Vajeeston, H. Fjellvåg, First-principles study of structural stability, dynamical and mechanical properties of Li_2FeSiO_4 polymorphs, RSC Adv. 7 (2017) 16843–16853. doi:10.1039/C6RA26555C.
[21] T. Matsushita, K. Mukai, Chemical thermodynamics in materials science, Springer Berlin Heidelberg, New York, NY, 2018. doi:10.1007/978-981-13-0405-7

Highlights

- $P2_1/n$ polymorph of Li_2FeSiO_4 was obtained by a solid state reaction at 750 °C.
- XRD analysis suggests exclusive occupation of Li2 crystallographic site by Fe as a result of antisite defect.
- Fe-Li2 interchange is energetically favorable over Fe-Li1 as confirmed by DFT calculations.